Hindawi
Journal of Electrical and Computer Engineering
Volume 2019, Article ID 4825787, 11 pages
https://doi.org/10.1155/2019/4825787

Research Article

Induction Motor Stator Interturn Short Circuit Fault Detection in Accordance with Line Current Sequence Components Using Artificial Neural Network

Gayatridevi Rajamany,[1,2] **Sekar Srinivasan**,[3] **Krishnan Rajamany**,[4] **and Ramesh K. Natarajan**[5]

[1]*Dept. of EEE, KCG College of Technology, Chennai, India*
[2]*Hindustan Institute of Technology and Science, Chennai, India*
[3]*Dept. of EEE, Hindustan Institute of Technology and Science, Chennai, India*
[4]*Dept. of BCA, Krupanidhi Degree College, Bangalore, India*
[5]*Mechatronics and Motion Systems, Bonfiglioli Transmissions Private Limited, Bologna, Italy*

Correspondence should be addressed to Gayatridevi Rajamany; gayatridevir@gmail.com

Received 10 July 2019; Revised 21 September 2019; Accepted 15 October 2019; Published 11 December 2019

Academic Editor: Alessandro Lidozzi

The intention of fault detection is to detect the fault at the beginning stage and shut off the machine immediately to avoid motor failure due to the large fault current. In this work, an online fault diagnosis of stator interturn fault of a three-phase induction motor based on the concept of symmetrical components is presented. A mathematical model of an induction motor with turn fault is developed to interpret machine performance under fault. A Simulink model of a three-phase induction motor with stator interturn fault is created for extraction of sequence components of current and voltage. The negative sequence current can provide a decisive and rapid monitoring technique to detect stator interturn short circuit fault of the induction motor. The per unit change in negative sequence current with positive sequence current is the main fault indicator which is imported to neural network architecture. The output of the feedforward backpropagation neural network classifies the short circuit fault level of stator winding.

1. Introduction

Induction motors overpower the field of electromechanical energy conversion. Their reliability, low cost, and high performance make them the most popular alternating current motors. These motors have the flexibility of being applied in various fields, from household appliances to high power industrial motors. In recent years, the problems of failure in large induction motors have become more significant. For the fault diagnosis problem, it is important to detect if the system has a fault and find its origin [1]. If motor failure is unattended at an early stage, it may become detrimental and damage the motor. This will cause industry production cessation.

In [2], many fault situations are mentioned. One among them is a case in which a disintegrated rotor bar had erupted from the slot and created damage in the stator winding. Faults in the induction motor can be either mechanical or electrical. Major mechanical faults are bearing fault [3–5] and broken rotor bar [6–10]. Electrical fault is influenced by power quality supplied by AC grid, frequency variations, voltage disturbances, and load variation. Another fault is short circuits stator winding [3, 11–14]. About more than one-third of the total fault occurring in the induction motor is that of stator winding fault. Short circuit in the stator winding takes very short time to evolve and totally damage the motor. Normally, the interturn short circuit fault progresses to an intercoil fault, phase winding fault, and single line ground fault, resulting in the breakdown of the motor. Detection of winding fault in the starting stage increases the practicability of repairing the machine by rewinding it or, in large motors, displacing short-circuited coils.

Traditional ways of fault monitoring were in regard to the leakage flux sensing [15], partial discharge [16], harmonics in stator current and voltage [17], etc. Ensuing studies, however, demonstrated that many of these traditional techniques are

liable to oddity due to supply voltage distortions [18], built in machine asymmetries [19], coincidental effects of the stator and rotor faults, etc. Motor current signature analysis (MCSA) is an important technique adopted for condition monitoring. Induction motor faults like bearing problems, broken rotor bar, eccentricity abnormalities, and stator winding faults cause variation in amplitude and frequency of motor current signature [3–9, 11–14].

A breakthrough in signal conditioning techniques and advances in computer software has taken machine fault detection to newer heights. Most of the demonstrated work in stator winding fault detection is from a frequency analysis domain. Signal transforming methods like fast Fourier transform (FFT), S-transform, short-time Fourier transform (STFT), wavelet transform, and Hilbert transforms have been adopted in combination with various classification techniques such as expert systems, artificial neural network, fuzzy logic, and support vector machine [20–26] for the motor degradation.

Eminent interest has been shown in [27–29] for artificial neural network in fault detection of the induction motor. The necessary condition to contrivance a successful ANN classifier is the selection of appropriate inputs about each case of fault. In [27, 28], stator interturn fault location detection by ANN is described considering frequency domain parameters as selected input.

In [29], ANN is applied for detecting the severity of the intercoil fault with the selected parameter from time domain. The work in [30–33] focuses on negative sequence current which is caused due to unbalanced windings.

Most of the research work in induction motor stator winding fault detection is from the analysis of the frequency domain. If we choose line currents or line voltages as parameters considered for fault detection, time domain analysis is also equally efficient. This will avoid usage of the spectral analyzer and sophisticated signal conditioning techniques, which makes the fault detection system unit much simpler. The aim is to identify a universal diagnostic technique to detect the winding fault and its severity level without motor constructional data and with knowledge of fault parameters from the time domain analysis.

In this work, we attempt to find a detection technique for stator winding fault based on per unit value of sequence components of current from time domain and classify the severity of fault by using artificial neural network. Here, network has been trained with a full range of input vector obtained from a Simulink model. NN input vector contains experimental values up to a feasible range and Simulink values to complete the input set. This provides a well-trained network. Simulation values are in close agreement with experimental values. Fault detection in the initial stage increases the viability of repairing the machine, and a nip in the bud avoids electrical spark and explosion.

Next session details mathematical modeling of the induction motor with stator winding fault. Using these mathematical equations, the model is created in Simulink which is described in Section 3. The classification method used for fault detection is emphasized in Section 4.

2. Mathematical Modeling of Stator Winding Turn Fault

A three-phase induction motor with turn fault in one-phase stator winding is considered, where β is the fraction of shorted turns. Winding in this phase has two parts—shorted turns and unfaulted turns. Machine equations in *abc* variables for a symmetrical motor with turn fault in one winding can be expressed as [34–36]. Here, we assumed that the leakage inductance of the shorted turns is βL_{ls}, where L_{ls} is the per-phase leakage inductance and the fault impedance is resistive R_f.

$$\begin{aligned} \mathbf{v}_s &= \mathbf{R}_s \mathbf{i}_s + \frac{\mathrm{d}\boldsymbol{\lambda}_s}{\mathrm{d}t}, \\ 0 &= \mathbf{R}_\gamma \mathbf{i}_\gamma + \frac{\mathrm{d}\boldsymbol{\lambda}_\gamma}{\mathrm{d}t}, \end{aligned} \tag{1}$$

where

$$\begin{aligned} \mathbf{v}_s &= \begin{bmatrix} v_{as1} & v_{as2} & v_{bs} & v_{cs} \end{bmatrix}^T, \\ \dot{i}_s &= \begin{bmatrix} i_{as} & \left(i_{as} - i_f\right) & i_{bs} & i_{cs} \end{bmatrix}, \\ \mathbf{i}_\gamma &= \begin{bmatrix} i_{a\gamma} & i_{b\gamma} & i_{c\gamma} \end{bmatrix}^T, \\ \boldsymbol{\lambda}_s &= \begin{bmatrix} \lambda_{as1} & \lambda_{as2} & \lambda_{bs} & \lambda_{cs} \end{bmatrix}^T \\ &= \mathbf{L}_{ss}\mathbf{i}_s + \mathbf{L}_{sr}\mathbf{i}_r, \\ \boldsymbol{\lambda}_r &= \begin{bmatrix} \lambda_{ar} & \lambda_{br} & \lambda_{cr} \end{bmatrix}^T \\ &= \mathbf{L}_{sr}^{\mathrm{T}}\mathbf{i}_s + \mathbf{L}_{rr}\mathbf{i}_r. \end{aligned} \tag{2}$$

The resistance matrices of equation (1) are as follows:

$$\begin{aligned} \mathbf{R}_s &= R_s \,\mathrm{diag}\begin{bmatrix} 1 & -\beta & \beta & 0 & 0 \end{bmatrix}, \\ \mathbf{R}_\gamma &= R_\gamma I_{3\times 3}. \end{aligned} \tag{3}$$

Adding the first two rows of equation (1),

$$\begin{aligned} v_s' &= R_s i_s + \frac{\mathrm{d}\lambda_s'}{\mathrm{d}t} + \beta \mathbf{A}_1 i_f, \\ 0 &= R_\gamma i_\gamma + \frac{\mathrm{d}\boldsymbol{\lambda}_\gamma}{\mathrm{d}t}, \end{aligned} \tag{4}$$

where

$$\begin{aligned} \mathbf{v}_s' &= \begin{bmatrix} v_{as} & v_{bs} & v_{cs} \end{bmatrix}^T, \\ \mathbf{i}_s' &= \begin{bmatrix} i_{as} & i_{bs} & i_{cs} \end{bmatrix}^T, \\ \boldsymbol{\lambda}_s' &= \begin{bmatrix} \left(\lambda_{as1} + \lambda_{as2}\right) & \lambda_{bs} & \lambda_{cs} \end{bmatrix}^T \\ &= \mathbf{L}_{ss}'\mathbf{i}_s' + \mathbf{L}_{sr}'\mathbf{i}_r + \beta \mathbf{A}_2 i_f, \\ \boldsymbol{\lambda}_\gamma &= \mathbf{L}_{sr}^{'T}\mathbf{i}_s' + \mathbf{L}_{\gamma\gamma}\mathbf{i}_\gamma + \beta \mathbf{A}_3 i_f, \\ \mathbf{A}_1 &= -\begin{bmatrix} R_s & 0 & 0 \end{bmatrix}^T, \\ \mathbf{A}_2 &= \begin{bmatrix} -\left(L_{ls} + L_{ms}\right) & \frac{L_{ms}}{2} & \frac{L_{ms}}{2} \end{bmatrix}^T, \\ \mathbf{A}_3 &= -L_{ms}\begin{bmatrix} \cos\theta_\gamma & \cos\left(\dot{\theta}_r + \frac{2\pi}{3}\right) & \cos\left(\theta_\gamma - \frac{2\pi}{3}\right) \end{bmatrix}^T. \end{aligned} \tag{5}$$

Inductance matrices are modified as

$$\mathbf{L}'_{ss} = \begin{bmatrix} L_{ls} + L_{ms} & -\frac{L_{ms}}{2} & -\frac{L_{ms}}{2} \\ -\frac{L_{ms}}{2} & L_{ls} + L_{ms} & -\frac{L_{ms}}{2} \\ -\frac{L_{ms}}{2} & -\frac{L_{ms}}{2} & L_{ls} + L_{ms} \end{bmatrix},$$

$$\mathbf{L}'_{sr} = L_{ms} * \begin{bmatrix} \cos\theta r & \cos\left(\theta r + \frac{2\pi}{3}\right) & \cos\left(\theta r - \frac{2\pi}{3}\right) \\ \cos\left(\theta r - \frac{2\pi}{3}\right) & \cos\theta r & \cos\left(\theta r + \frac{2\pi}{3}\right) \\ \cos\left(\theta r + \frac{2\pi}{3}\right) & \cos\left(\theta r - \frac{2\pi}{3}\right) & \cos\theta r \end{bmatrix}. \tag{6}$$

The voltage and flux linkage equations for the shorted turns (β_{s2}) are

$$V_{as2} = \beta R_s\left(i_{as} - i_f\right) + \frac{\mathrm{d}\lambda_{as2}}{\mathrm{d}t} = R_f i_f,$$
$$\lambda_{as2} = -\beta A_2^T i'_s - \beta A_3^T i_\gamma - \beta\left(L_{ls} + \beta L_{ms}\right) i_f. \tag{7}$$

The expression of electromagnetic torque can be in machine *abc* variables is

$$T = \frac{P}{2} i_s^T \frac{\partial \mathbf{L}_{sr}}{\partial \theta_\gamma} \mathbf{i}_\gamma. \tag{8}$$

The inductance matrices are given by (9)–(11)

$$\mathbf{L}_{ss} = L_{ls}\mathrm{diag}\left[\,1 \;\; -\beta \;\; \beta \;\; 0 \;\; 0\,\right] + L_{ms}\begin{bmatrix} 1-\beta^2 & \beta 1-\beta & -\frac{1-\beta}{2} & -\frac{1-\beta}{2} \\ \beta 1-\beta & \beta^2 & -\frac{\beta}{2} & -\frac{\beta}{2} \\ \frac{-(1-\beta)}{2} & -\frac{\beta}{2} & 1 & \frac{-1}{2} \\ -\frac{1-\beta}{2} & -\frac{\beta}{2} & -\frac{1}{2} & 1 \end{bmatrix}, \tag{9}$$

$$\mathbf{L}_{sr} = L_{ms}\begin{bmatrix} 1-\beta\cos\theta_\gamma & 1-\beta\cos\theta_\gamma + \frac{2\pi}{3} & 1-\beta\cos\theta_\gamma - \frac{2\pi}{3} \\ \beta\cos\theta_\gamma & \beta\cos\theta r + \frac{2\pi}{3} & \beta\cos\theta r - \frac{2\pi}{3} \\ \cos\theta r - \frac{2\pi}{1} & \cos\theta r & \cos\theta r + \frac{2\pi}{3} \\ \cos\theta r + \frac{2\pi}{1} & \cos\theta r - \frac{2\pi}{3} & \cos\theta r \end{bmatrix}, \tag{10}$$

$$\mathbf{L}_{rr} = \begin{bmatrix} L_{lr} + L_{ms} & \frac{-L_{ms}}{2} & \frac{-L_{ms}}{2} \\ \frac{-L_{ms}}{2} & L_{lr} + L_{ms} & \frac{-L_{ms}}{2} \\ \frac{-L_{ms}}{2} & \frac{-L_{ms}}{2} & L_{lr} + L_{ms} \end{bmatrix}. \tag{11}$$

3. Sequence Component Analysis and Parameter Extraction

The symmetrical components are solid tool for analyzing and solving the problems of any unbalanced system. The symmetrical components are found reliable indicators of stator turn faults. By principle, symmetrical (without fault) motors supplied with symmetrical three-phase voltage sources will not produce negative sequence currents. When a turn fault occurs, symmetry will disturb and generate negative and zero sequence currents. In reference to the symmetrical components practice, three sets of symmetrical balanced phases are derived from any set of unbalanced parameters. They are recognized as positive, negative, and zero sequence components. Using Fortescue's transformation given by equation (12), symmetrical components (I_P, I_N, I_0) are calculated from unbalanced phase currents (I_a, I_b, I_c).

$$\begin{bmatrix} I_P \\ I_N \\ I_0 \end{bmatrix} = \frac{1}{3}\begin{bmatrix} 1 & a & a^2 \\ 1 & a^2 & a \\ 1 & 1 & 1 \end{bmatrix}\begin{bmatrix} I_a \\ I_b \\ I_c \end{bmatrix}, \tag{12}$$

where a = operator $e^{j(2\pi/3)}$.

Fundamentally, the three-phase induction motor is a symmetrical system in healthy conditions and produces only positive sequence currents. It generates positive, negative, and zero sequence when symmetry is disturbed during a fault situation.

MATLAB software is used for creating a simulation model of a three-phase motor with turn fault in one of the phase winding. Due to the difficulty in creating the fault and measuring the phase currents experimentally for high values of percentage shorting, we are forced to create the Simulink model. Simulink of the induction motor with stator winding shorting is constructed based on the fundamental equations mentioned in Section 2. The Simulink model of the motor with interturn short is shown in Figure 1.

The model is simulated for different levels of shorting in one-phase winding and values of phase currents are saved in the MATLAB workspace. From these values, negative sequence current, positive sequence current, and zero sequence currents are calculated. Phase currents and sequence currents for different fault levels are tabulated in Table 1.

Here, simulation is carried out by introducing short circuiting in one phase at a time. The severity level of fault has been increased from zero percentage gradually. A negative sequence component of current is found to be increasing gradually with an increase in the fault level.

The Simulink data are verified by conducting experiments on three-phase induction motors rated 5 hp and 1 hp. Three-phase induction motors of Kirloskar electric company having specification 5 hp, 1430 rpm, 415 V, and 10 A and a digital oscilloscope-DS 1150 are used in the experiment. The experimental setup of stator interturn fault is shown in Figure 2. Interturn short circuit is created by taking out tapings from one of the phase windings. Table 2 gives the comparison of phase current values of winding with shorted turns from experimental setup and that from the Simulink model of the same rated motor.

Experimental values and simulated values are comparable since error percentage of both values is very low, thus proving the authenticity of the Simulink model.

For 5 hp motor, current values obtained practically are compared with those obtained from the mathematical model, described under Section 2. The details of winding parameters used for calculation are

Stator resistance, $R_s = 0.2777\ \Omega$

Rotor resistance, $R_r = 0.183\ \Omega$

Stator inductance, $L_s = 0.0553$ H

Rotor inductance, $L_r = 0.056$ H

Mutual inductance, $L_m = 0.0538$ H

Error percentage of simulation values with mathematical model values listed in Table 3 is very low. Comparison output shows compliance or proves the validity of the Simulink model.

Simulated values are compared with practical values as well as analytical values from a mathematical model. Mean Error percentage of phase current values obtained from experiment and simulation are 0.00249. Mean error percentage of simulated values with analytical values of the mathematical model is 0.0051. The comparison output shows compliance and proves the validity of Simulink model.

The per unit change in a negative sequence current with positive sequence current is considered as the main input parameter for classification of severity of the fault level in phase windings.

$$\boldsymbol{\delta} = \frac{(\text{positive sequence current} - \text{negative sequence current})}{\text{positive sequence current}},$$

$$\boldsymbol{\delta} = \frac{(\mathbf{I}_P - \mathbf{I}_N)}{\mathbf{I}_P}. \tag{13}$$

Case 1: with zero percentage shorting (healthy)

$I_{\text{negative}} = 0$
$I_{\text{positive}} = 10.0248$
And so $\delta = 1$

Case 2: turn fault of 1.4 percentage

$I_{\text{negative}} = 0.0254$
$I_{\text{positive}} = 10.0493$
$\delta = (10.0493 - 0.0254)/10.0493 = 0.997472461$

The value of δ for various levels of short circuiting is tabulated in Table 4. Selection of effective parameter is very important in fault detection along with the selection of classifier.

Generalization capacity of fault indicator parameter (δ) has been checked for five motors. The specifications of motors (I to V) considered for analysis are

M I- 1.1 KW, 400 V, 50 Hz, 1447 rpm, 2.7 A

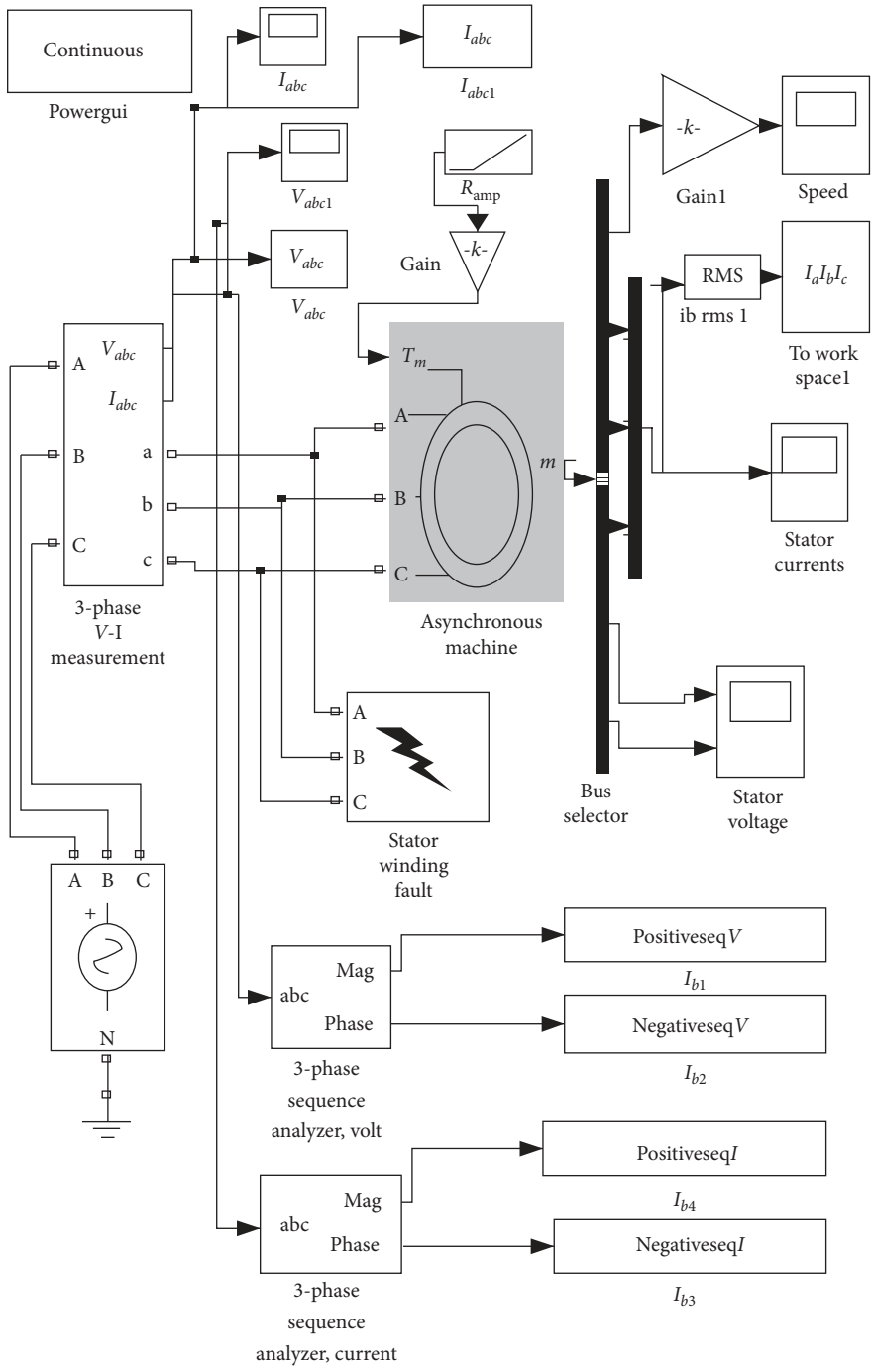

Figure 1: Simulink model for extraction of sequence components of current and voltage.

M II- 5.5 KW, 400 V, 50 Hz, 1457 rpm, 11.6 A

M III- 55 KW, 400 V, 50 Hz, 1480 rpm, 102 A

M IV-110 KW, 400 V, 50 Hz, 1487 rpm, 194 A

M V-250 KW, 400 V, 50 Hz, 1488 rpm, 445 A

The value of δ varies from 1 to 0.95 for short circuit levels 0% to 15%. In this case, the input vector to NN or fault indicator values ($\boldsymbol{\delta}$) is identical for all motors for a specific fault level. Figure 3 shows the variation of δ values at different interturn fault levels for motors under analysis.

4. Neural Network for Classification

Artificial neural networks are indulgent to noise and respond quickly, so they can be employed in real-time fault detection [27–29]. Since it is not possible to create a look-up table storing data for all conditions, a feedforward neural network is used for classifying the fault. Anticipating maximum accuracy from the trained neural network, input vector is created using possible experimental values and Simulink values for high percentage shorting. The various processes involved in the work of detection of severity level

Table 1: Magnitude of phase currents and sequence components of phase currents.

% shorting in phase-A winding	Phase current values (A)			Sequence component of current values		
	I_a	I_b	I_c	$I_{positive}$	$I_{negative}$	I_{zero}
0	10.1651	10.162	10.165	10.0248	0	0
0.233	10.252	10.17	10.1705	10.0289	0.0042	0.0043
0.467	10.339	10.17	10.1705	10.0329	0.0085	0.0085
0.7	10.4259	10.17	10.1705	10.037	0.0127	0.0127
0.933	10.5129	10.17	10.1705	10.0411	0.0169	0.0169
1.167	10.5998	10.17	10.1705	10.0452	0.0212	0.0212
1.4	10.6867	10.17	10.1705	10.0493	0.0254	0.0254
1.633	10.7737	10.17	10.1703	10.0534	0.0296	0.0296
1.867	10.8606	10.17	10.1703	10.0574	0.0338	0.0339
2.1	10.9476	10.17	10.1703	10.0615	0.0381	0.0381
2.333	11.0345	10.17	10.1705	10.0656	0.0423	0.0423
3.5	11.1932	10.17	10.1704	10.1074	0.0862	0.0862
4.667	11.3508	10.17	10.1704	10.1498	0.1309	0.1309
5.833	11.5174	10.17	10.1704	10.1951	0.1784	0.1784
7	11.6899	10.17	10.1704	10.2406	0.2255	0.2255
8.167	11.8631	10.17	10.1704	10.2859	0.2737	0.2737
9.333	12.0455	10.17	10.1702	10.3337	0.3238	0.3238
10.5	12.2366	10.17	10.1702	10.3825	0.3755	0.3755

Figure 2: Experimental setup of 5 hp three-phase induction motor with interturn fault in one phase.

Table 2: Comparison of phase current values of 5 hp motor obtained from simulation and experiment.

S. no	Fault % in phase-A winding	Phase current values (A) obtained from		Error percentage
		Experiment	Simulation	
1	0	10.2	10.1651	0.0034216
2	0.7	10.4	10.4259	−0.0024904
3	1.4	10.7	10.6867	0.00124299
4	2.1	10.9	10.9476	−0.00436697
5	3.5	11.2	11.1932	0.000607142
6	7	11.7	11.6899	0.000901785
7	10.5	12.2	12.2366	−0.00300
8	15	12.6	12.6254	−0.00201587

Table 3: Comparison of phase current values of 5 hp motor obtained from experiment and mathematical model.

S. no	β (fraction of shorted turns)	Phase current values (A)		Error percentage
		Mathematical model	Simulation	
1	0.007	10.386	10.4259	−0.00384171
2	0.014	10.695	10.6867	0.007760636
3	0.021	10.921	10.9476	−0.002435674
4	0.035	11.193	11.1932	−0.001786831
5	0.07	11.684	11.6899	−0.00504964
6	0.105	12.243	12.2366	0.0005227477
7	0.15	12.630	12.6254	0.0036421219
8	0.18	12.828	12.832	−0.00311817

Table 4: Calculated parameter values.

S. no	Percentage shorting in phase-winding	$\boldsymbol{\delta} = [\mathbf{I}_{positive} - \mathbf{I}_{negative}]/\mathbf{I}_{positive}$
1	0	1
2	0.233	0.99958121
3	0.467	0.999152787
4	0.7	0.998734682
5	0.933	0.998316917
6	1.167	0.997889539
7	1.4	0.997472461
8	1.633	0.997055722
9	1.867	0.99663929
10	2.1	0.996213288
11	2.333	0.995797568
12	3.5	0.991471595
13	4.667	0.987103194
14	5.833	0.982501398
15	7	0.977979806
16	8.167	0.973390758
17	9.333	0.968665628
18	10.5	0.963833373

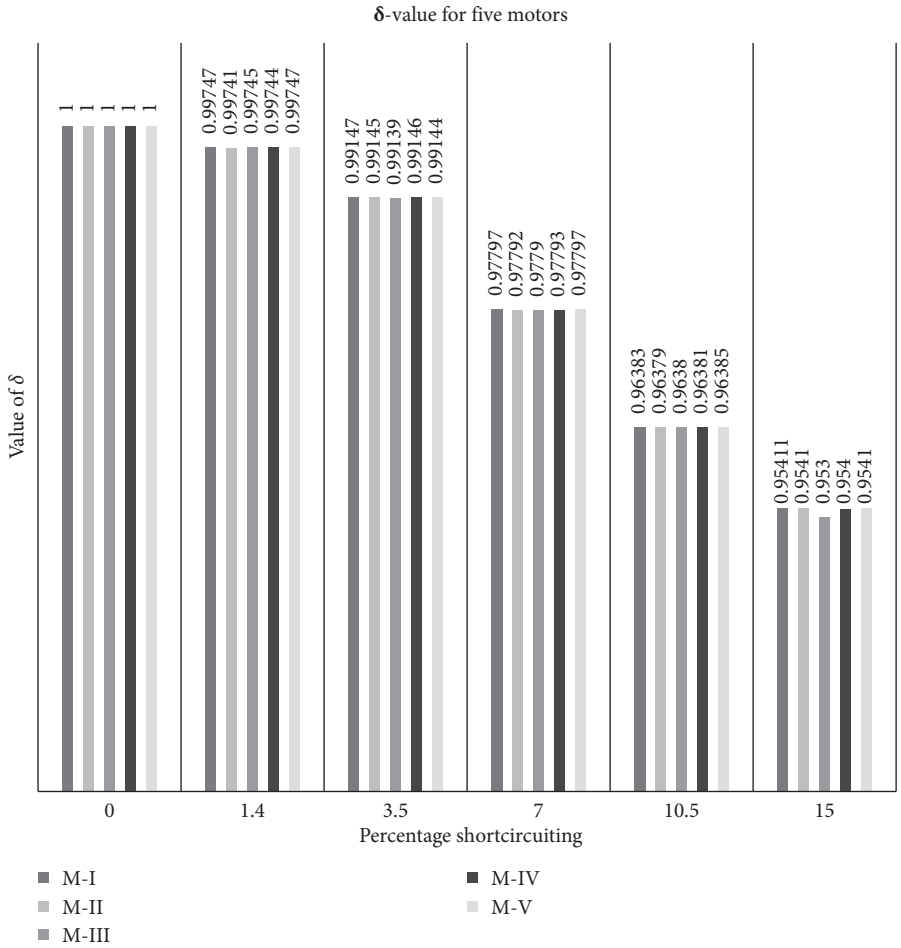

Figure 3: Variation of δ values at different interturn fault levels for motors (M-I to M-V).

of shorting in stator winding are described in the block diagram (Figure 4).

The design and development of neural networks comprises preparation of input data set for the neural network, selection of a network structure, training of the network, testing, and evaluation of the classifier.

Backpropagation (BP), which is the most popular supervised learning method, is adopted for this process. This

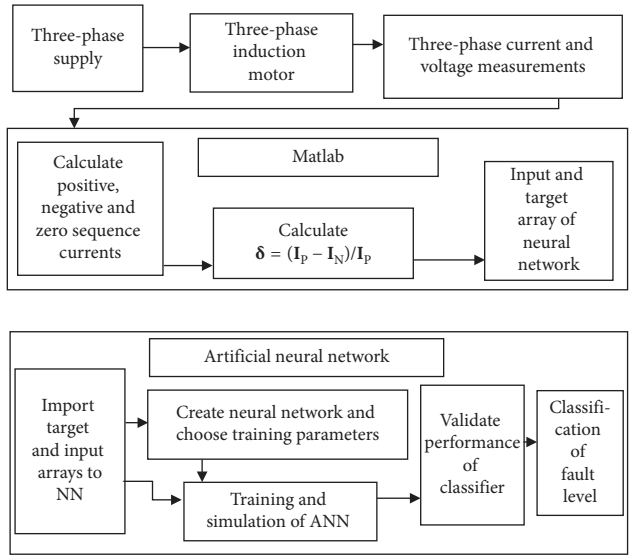

Figure 4: Block diagram of processes.

Table 5: Input and target values for ANN.

$X = (I_{positive} - I_{negative})/I_{positive}$	ANN classifier target value	% shorting/severity level
1	10000	0
0.99958121	10023	0.233
0.999152787	10046	0.467
0.998734682	10070	0.7
0.998316917	10093	0.933
0.997889539	10116	1.167
0.997472461	10140	1.4
0.997055722	10163	1.633
0.99663929	10186	1.867
0.996213288	10210	2.1
0.995797568	10233	2.333
0.991471595	10350	3.5
0.987103194	10466	4.667
0.982501398	10583	5.833
0.977979806	10700	7
0.973390758	10816	8.167
0.968665628	10933	9.333
0.963833373	11050	10.5
0.959022445	11166	11.667
0.95449383	11333	13.333
0.954113909	11500	15
0.954000839	11667	16.667
0.948959154	11800	18
0.943823196	11916	19.167
0.938604651	12033	20.334

learning algorithm increases the efficiency of the network by minimizing the error, and so the gradient of the error curve slopes down.

The input data to NN are array of δ values. Target value is fixed for each value of input, δ. Both input data and target values for different classification levels are displayed in Table 5. Data set for training is selected in such a way that it contains the actual practical values till maximum measurable value during short circuiting and full range of values from simulation.

Target value [10000] represents healthy condition of winding. Target value is fixed as 1xxxx where xxxx represents xx.xx% level of shorting. Target for 00.23% of severity is 10023, for 01.40% of severity is 10140 and for 23.17% severity is 12317.

The performance of the algorithm is sensitive to the setting of the learning rate. A very small learning rate will lead to longer converging time, and a very high learning rate can lead to oscillating and unstable algorithm.

Backpropagation training with an adaptive learning rate is implemented with gradient descent function. Hyperbolic

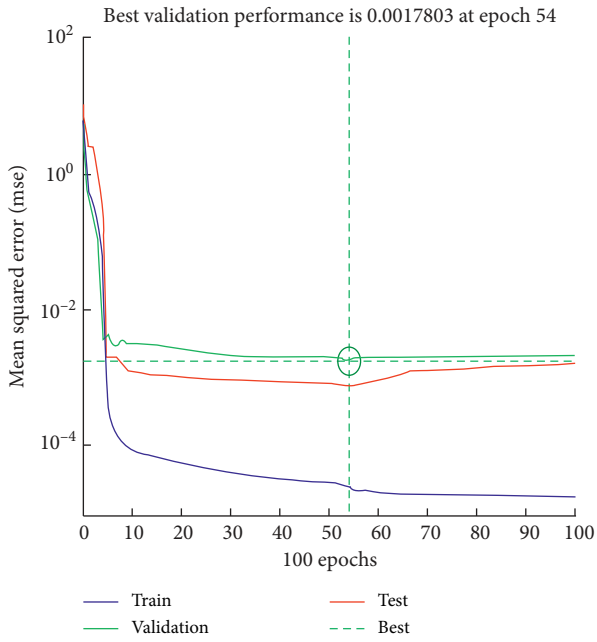

Figure 5: Performance plot of trained network.

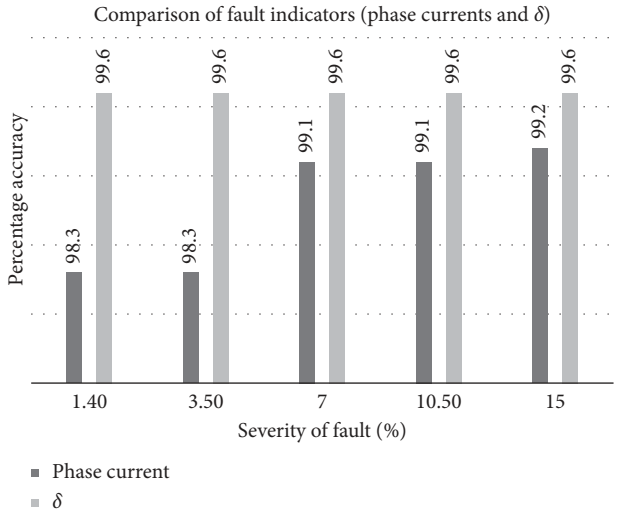

Figure 6: Comparison between fault indicators.

tangent sigmoid transfer function is used, which calculates a layer's output from its net input. Mean squared normalized error performance function measures the network performance according to the mean of squared errors, when incorporated into the training process enhances the efficiency of the synaptic weight's adjustment. A very low MSE reflects that the desired output and the ANNs outputs are close to each other, and thereby the network is well trained.

5. Result and Performance Validation

The proposed networks were subjected to training with input signals as described in Section 4. While analyzing the performance and regression plot of networks, it has been found that neural networks reacted well with training and validation samples. Validation performance of the network gave 100% accuracy (with 50 samples). So, accuracy percentage is calculated with error between target value and actual output vector. The level of accuracy obtained is 99.05%. The performance plot of the neural network is given in Figure 5 Stopping criterion is established with means squared error of $1.02e-005$.

NN with 2 hidden layers and number neurons in hidden layers as 16 and 1, respectively, shows the highest accuracy of 99.6%.

Comparison is made between the performance of neural networks which are fed with three-phase currents as input and $\boldsymbol{\delta}$ as input. Neural network with $\boldsymbol{\delta}$ as input vector shows steady increase in percentage accuracy. The graph in Figure 6 shows the percentage accuracy of the neural network when it is trained with phase currents as input vector and when trained with proposed fault indicator $\boldsymbol{\delta}$ as input vector where, $\boldsymbol{\delta} = (\mathbf{I}_P - \mathbf{I}_N)/\mathbf{I}_P$.

6. Conclusion

This research focus is to make progress as well as to simplify the field of condition monitoring and fault detection in an induction motor. Negative sequence current monitoring is one of the simplest but solid and substantial techniques for stator short circuit detection. It is relevant to specify that selection of fault indicator is very critical in the classification process. In this work, per unit change in a negative sequence current with positive sequence current is considered as the fault indicator and so found to be more generalized technique for interturn stator winding fault detection. While phase current is considered as fault indicator, input vector of NN is different for different motors. When taken δ as fault indicator, input vector of NN is the same for different motors because of its per unit nature.

The fault parameter under consideration is derived from the time domain, which avoids the use of sophisticated signal conditioning techniques used in frequency domain for fault detection.

The work presents an application of neural network to classify the stator interturn fault. The network is trained with a full range of input vector using experimental values (for a small level of fault) as well as Simulink values (for high level of fault). Thus, NN is well trained with a full range of data sets. Simulink modeling helps create an infinite database, which is not possible by means of experiment. The performance of the NN is found to be accurate and fast. Fault detection in the beginning stage increases the feasibility of repairing the machine and avoids the risk of fire and explosion. Future extension of NN is possible to account detection of other electrical and mechanical faults possible in an induction motor.

Data Availability

The Simulink model data used for parameter calculation and the neural network training and testing data used to support the findings of this study are included within the article.

Consolidated data, which are used for checking the generalization of five different motors, are included within the article.

Conflicts of Interest

The authors declare that they have no conflicts of interest.

Acknowledgments

This work was carried out in state-of-the-art Power System Protection Laboratory, Department of Electrical and Electronics, KCG College of Technology, Chennai, India. The lab is established under FIST (Fund for Improvement of S&T Infrastructure) scheme, supported by the Department of Science and Technology (DST), Government of India.

References

[1] M. Y. Chow, "Guest editorial special section on motor fault detection and diagnosis," *IEEE Transactions on Industrial Electronics*, vol. 47, no. 5, pp. 982-983, 2000.

[2] W. T. Thomson and R. J. Gilmore, "Motor current signature analysis to detect faults in induction motor drives," in *Proceedings of the Thirty Second Turbo Machinery Symposium*, pp. 145–156, Houston, TX, USA, September 2003.

[3] H. Jafari and J. Poshtan, "Fault detection and isolation based on fuzzy-integral fusion approach," *IET Science, Measurement & Technology*, vol. 13, no. 2, pp. 206–302, 2019.

[4] R. Sadeghi, H. Samet, and T. Ghanbari, "Detection of stator short-circuit faults in induction motors using the concepts of instantaneous frequency," *IEEE Transactions on Industrial Informatics*, vol. 15, no. 8, pp. 4506–4515, 2019.

[5] G. S. Maruthi and V. Hedge, "Application of MEMS accelerometer for detection and diagnosis of multiple faults in the roller element bearings of three phase induction motor," *IEEE Sensors Journal*, vol. 16, no. 1, pp. 145–152, 2016.

[6] Y. Soufi, T. Bahi, M. F. Harkat, and M. Mahammedi, "fault diagnosis methods for three phase PWM inverter fed induction motor," *International Journal on Engineering Applications*, vol. 6, no. 4, pp. 101–112, 2018.

[7] T. G. Luis Alonso, M. Johnny Rodriguez, M. A. Moonem, and M. A. Platas-Garza, "A multiresolution Taylor–Kalman approach for broken rotor bar detection in cage induction motors," *IEEE Transactions on Instrumentation and Measurements*, vol. 67, no. 6, pp. 1317–1328, 2018.

[8] G. Mirzaeva and K. Saad, "Advanced diagnosis of stator turn-to-turn faults and static eccentricity in induction motors based on internal flux measurement," *IEEE Transactions on Industry Applications*, vol. 54, no. 4, pp. 3961–3970, 2018.

[9] A. Naha, A. K. Samanta, A. Routray, and A. K. Deb, "A method for detecting half-broken rotor bar in lightly loaded induction motors using current," *IEEE Transactions on Instrumentation and Measurements*, vol. 65, no. 7, pp. 1614–1625, 2016.

[10] J. Zarei, M. Mehdi Arefi, and H. Hassani, "Bearing fault detection based on interval type-2 fuzzy logic systems for support vector machines," in *Proceedings of the 6th International Conference on Modelling, Simulation and Applied Optimization (ICMSAO)*, Istanbul, Turkey, May 2015.

[11] D. G. Dorrell and K. Makhoba, "Detection of inter-turn stator faults in induction motors using short-term averaging of forward and backward rotating stator current phasors for fast prognostics," *IEEE Transactions on Magnetics*, vol. 53, no. 11, pp. 1–7, 2017.

[12] H. Abdallah and K. Benatman, "Stator winding inter-turn short-circuit detection in induction motors by parameter identification," *IET Electric Power Applications*, vol. 11, no. 2, pp. 272–288, 2017.

[13] B. Gustavo Henrique, S. Paulo Rogerio, E. Wagner, A. Goedtel, R. H. C. Palacios, and W. F. Godoy, "Stator short-circuit diagnosis in induction motors using mutual information and intelligent systems," *IEEE Transactions on Industrial Electronics*, vol. 66, no. 4, pp. 3237–3246, 2019.

[14] M. Ojaghi, M. Sabouri, and J. Faiz, "Performance analysis of squirrel-cage induction motors under broken rotor bar and stator inter-turn fault conditions using analytical modeling," *IEEE Transactions on Magnetics*, vol. 54, no. 11, pp. 1–5, 2018.

[15] H. Dehghan, F. Haghjoo, and S. M. A. Cruz, "A flux-based differential technique for turn-to-turn fault detection and defective region identification in line -connected and inverter-fed induction motors," *IEEE Transactions on Energy Conversion*, vol. 33, no. 4, pp. 1876–1885, 2018.

[16] I. Jeftenic, N. Kartalovic, D. Brajovic, and B. Loncar, "Aging of stator coil interconductor insulation of high voltage asynchronous motor," *IEEE Transactions on Dielectrics and Electric Insulation*, vol. 25, no. 1, pp. 352–359, 2018.

[17] S. T. Lee and H. Jin, "Detection technique for stator inter-turn faults in BLDC motors based on third harmonic components of line currents," *IEEE Transactions on Industry Applications*, vol. 53, no. 1, pp. 143–150, 2017.

[18] A. H. Bonnett and G. C. Soukup, "Cause and analysis of stator and rotor failures in three phase squirrel cage induction motors," *IEEE Transactions Industry Applications*, vol. 28, no. 4, pp. 921–937, 1992.

[19] G. B. Kliman, W. J. Premelani, and R. A. Koeg, "A new approach to online turn fault detection in AC motors," in *Proceedings of the Conference Record of the 1996 IEEE Industry Applications Conference Thirty-First IAS Annual Meeting (IAS '96)*, vol. 1, pp. 687–693, San Diego, CA, USA, October 1996.

[20] H. Hassani, J. Zarei, M. Mehdi Arefi, and R. Razavi-Far, "zSlices-based general type-2 fuzzy fusion of support vector machines with application to bearing fault detection," *IEEE Transactions on Industrial Electronics*, vol. 64, no. 9, pp. 7210–7217, 2017.

[21] A. P. Mittal, H. Malik, S. Rastogi, and V. Talur, "External fault identification by 3-phase induction motor using PSVM," in *Proceedings of the 6th IEEE Power India International Conference (PIICON)*, Delhi, India, June 2015.

[22] Z. Zhang, L. Gu, and Y. Zhu, "Intelligent fault diagnosis of rotating machine based on SVMs and EMD method," *The Open Automation and Control Systems Journal*, vol. 7, no. 1, pp. 219–230, 2015.

[23] I. Bandyopadhyay, P. Purkait, and C. Koley, "Performance of a classifier based on time-domain features for incipient fault detection in inverter drives," *IEEE Transactions on Industrial Informatics*, vol. 15, no. 1, pp. 3–14, 2019.

[24] M. Z. Ali, M. N. S. K. Shabbir, X. Liang, Y. Zhang, and T. Hu, "Machine learning-based fault diagnosis for single- and multi-faults in induction motors using measured stator currents and vibration signals," *IEEE Transactions on Industry Applications*, vol. 55, no. 3, pp. 2378–2391, 2019.

[25] F. Ben Abid, S. Zgarni, and B. Ahmed, "Distinct bearing faults detection in induction motor by a hybrid optimized SWPT and aiNet-DAG SVM," *IEEE Transactions on Energy Conversion*, vol. 33, no. 4, pp. 1692–1699, 2018.

[26] W. Sun, R. Zhao, R. Yan, S. Shao, and X. Chen, "Convolutional discriminative feature learning for induction motor

fault diagnosis," *IEEE Transactions on Industrial Informatics*, vol. 13, no. 3, pp. 1350–1359, 2017.

[27] M. Bouzid, G. Champenois, N. M. Bellaj, L. Signac, and K. Jelassi, "An effective neural approach for the automatic location of stator inter-turn faults in induction motor," *IEEE Transactions on Industrial Electronics*, vol. 55, no. 12, pp. 4277–4289, 2008.

[28] X. Zhao, C. Hu, F. Yang et al., "Data-driven inter-turn short circuit fault detection in induction machines," *IEEE Access*, vol. 5, pp. 25055–25068, 2017.

[29] G. Rajamany and S. Srinivasan, "An artificial neural networks application for the automatic detection of severity of stator inter coil fault in three phase induction motor," *Journal of Electrical Engineering and Technology*, vol. 12, no. 6, pp. 2219–2226, 2017.

[30] R. M. Tallam, S. B. Lee, G. C. Stone et al., "A survey of methods for detection of stator-related faults in induction machines," *IEEE Transactions on Industry Applications*, vol. 43, no. 4, pp. 920–928, 2007.

[31] P. Ostojic, A. Banerjee, D. C. Patel, W. Basu, and S. Ali, "Advanced motor monitoring and diagnostics," *IEEE Transactions on Industry Applications*, vol. 50, no. 5, pp. 3120–3127, 2014.

[32] S. Samanta, J. N. Bera, and G. Sarkar, "Inter-turn fault diagnosis of three phase induction motor using SST and KNN," in *Proceedings of the Michael Faraday IET International Summit: MFIIS-Kolkata*, Kolkata, India, September 2015.

[33] D. G. Dorrell and K. Makhoba, "Detection of inter-turn stator faults in induction motors using short term averaging of forwards and backwards rotating stator current phasors for fast prognostics," in *Proceedings of the 2017 IEEE International Magnetics Conference (INTERMAG)*, vol. 53, no. 11, pp. 225–301, Dublin, Ireland, April 2017.

[34] M. Wieczorek and E. Rosolowski, "Modelling of induction motor for simulation of internal fault," in *Proceedings of the International Symposium on Modern Electric Power Systems (MEPS)*, Wroclaw, Poland, September 2010.

[35] D. A. Asfani, P. P. S. Saputra, I. M. Yulistya Negara, I. G. N. Satriyadi Hernanda, and R. Wahyudi, "Simulation analysis on high impedance temporary short circuit in induction motor winding," in *Proceedings of the International Conference on Quality in Research*, Yogyakarta, Indonesia, June 2013.

[36] H. Mahmoud, A.-E. Ahmed, N. Bianchi, S. M. El-Hakim, A. Shaltout, and L. Dupre, "An inverse approach for inter-turn fault detection in asynchronous machines using magnetic pendulous oscillation technique," *IEEE Transactions on Industry Applications*, vol. 52, no. 1, pp. 226–233, 2016.